Powder Metallurgy

Development of a new model describing the anisotropic dimensional change on sintering

--Manuscript Draft--

Manuscript Number:	
Full Title:	Development of a new model describing the anisotropic dimensional change on sintering
Short Title:	A new model of the anisotropic dimensional change on sintering
Article Type:	Research Article
Keywords:	dimensional change; anisotropy
Corresponding Author:	Alberto Molinari University of Trento TRENTO, ITALY
Corresponding Author Secondary Information:	
Corresponding Author's Institution:	University of Trento
Corresponding Author's Secondary Institution:	
First Author:	Alberto Molinari
First Author Secondary Information:	
Order of Authors:	Alberto Molinari
	Ilaria Cristofolini
	Marco Zago
	Onur Utku Uçak
	Bruno Vicenzi
	Mark James Dougan
	Markus Schneider
	Peter Hedegard Pedersen
	Johanna Bolitschek
	Juergen Voglhuber
Order of Authors Secondary Information:	
Abstract:	The anisotropic dimensional changes during sintering was investigated for rings made of eight different materials with different green densities and H/(Dext-Dint) ratio. Dimensional changes are affected by green density, as shown in previous works, while the geometrical parameter does not display a clear influence. The anisotropy parameter K defined in a previous work does not describe anisotropy of dimensional change unambiguously, due to the anisotropy of shrinkage/swelling in the compaction plane. A new anisotropy parameter (K3D) was therefore defined considering the dimensional changes of internal diameter, external diameter, and height. This parameter display an unambiguous dependence on the equivalent isotropic dimensional change and will be used in further work to develop a predictive model for the prediction of the anisotropic dimensional change during sintering of parts with different green density and geometry.
Funding Information:	

Development of a new model describing the anisotropic dimensional change on sintering

Ilaria Cristofolini[1], Alberto Molinari[1], Marco Zago[1], Onur Utku Uçak[1], Bruno Vicenzi[2], Mark James Dougan[3], Markus Schneider[4], Peter Hedegard Pedersen[5], Johanna Bolitschek[6], Juergen Voglhuber[6]

[1] University of Trento - Trento – Italy

[2] EPMA - Chantilly – France

[3] AMES Barcelona Sintering S.A.- Sant Vicenç dels Horts, B – Spain

[4] GKN Sintermetals GmbH - Radevormwald – Germany

[5] Sintex a/s - Hobro - Denmark

[6] Miba Sinter Austria GmbH - Vorchdorf – Austria

Abstract

The anisotropic dimensional changes during sintering was investigated for rings made of eight different materials with different green densities and H/(D_{ext}-D_{int}) ratio. Dimensional changes are affected by green density, as shown in previous works, while the geometrical parameter does not display a clear influence. The anisotropy parameter K defined in a previous work does not describe anisotropy of dimensional change unambiguously, due to the anisotropy of shrinkage/swelling in the compaction plane. A new anisotropy parameter (K_{3D}) was therefore defined considering the dimensional changes of internal diameter, external diameter, and height. This parameter display an unambiguous dependence on the equivalent isotropic dimensional change and will be used in further work to develop a predictive model for the prediction of the anisotropic dimensional change during sintering of parts with different green density and geometry.

Keywords: dimensional change; anisotropy.

1. Introduction

It is well-known that dimensional changes (shrinking/swelling) during sintering of prior cold compacted parts are anisotropic. This makes the design of the press and sinter process rather

complex and reduces the dimensional and geometrical precision of the products if it is not taken into consideration in the design of the compaction tools and strategy [1].

The origin of anisotropy in dimensional change during sintering has been investigated in several studies and different models has been developed. Wakai et al., attributed the anisotropic shrinkage of loose powders to the anisotropic sintering driving force and viscosity [2,3]. Olevsky correlated the anisotropic shrinkage of a prior cold compacted powder to the orientation of pores in the green microstructure [4]. Using the same model, Torresani et al. introduced the anisotropy of the mass transfer responsible for the neck growth and the dimensional change during sintering [5]. Zavaliangos et al. attributed the anisotropic shrinkage to the preferential orientation of metallic powders caused by the uniaxial cold compaction [6,7].

Other authors propose a correlation between the anisotropic stress field during uniaxial cold compaction and anisotropic shrinkage [8,9]. Powders are anisotropically deformed in the green part and both the geometrical and the structural condition of the powder promote an anisotropic dimensional change during the heating and the isothermal holding at the sintering temperature [10].

While above-mentioned works focus on investigating the mechanisms causing the anisotropic dimensional changes, some studies focus on dimensional changes and variables affecting these changes. Cristofolini et al. demonstrated that the shrinkage in the compaction plane is lower than that in compaction direction for parts produced with a Fe-Cu-P alloy [1], with a 3%Cr-0.5%Mo steel [11,12], and with a 1.5%Cr-0.2%Mo steel [13]. Cristofolini et al. [14] found that in liquid phase sintering of Cu steels swelling in the compaction plane is larger than that along the compaction direction [14]. This result confirms what reported by Wanibe et al. in their study of Fe-Cu parts [15]. Effect of Cu content on dimensional behavior of Fe-Cu-C parts is highlighted by Griffo et al [16]: when copper content is lower than 4%, radial swelling is greater than the axial one, while the opposite occurs when Cu>4%. Raman et al. demonstrated that swelling in the compaction plane is larger than that in axial direction [17]. Danninger showed that effect of liquid phase is insignificant on the anisotropy of dimensional change of Mo alloyed steels [18].

Dimensional change and its anisotropy depend on the geometry of the parts, too. Cristofolini et al. performed an experimental study using five axisymmetric parts and four different materials, and they proposed a model, correlating the anisotropy of dimensional changes to the material and the geometry of the parts [19]. Based on that study, a design methodology accounting for the

anisotropic dimensional change was proposed and validated in the frame of an EPMA Club Project involving several industrial partners [20,21]. The key element of the procedure is the definition of an anisotropy coefficient and its dependence on the equivalent isotropic dimensional change, collected in a database containing the dimensional changes of parts with different geometries and made of different materials. The procedure demonstrated the possibility to predict the anisotropic dimensional change of parts with quite a good precision, which can be improved expanding the database, including a greater number of materials and geometries. This is the aim of the present work. Eight different materials were used to produce ring-shaped parts with different dimensions and green densities. Materials were selected to investigate both the shrinking and the swelling systems, also both solid phase and liquid phase sintering processes. The parts were cold compacted, and sintered by the industrial partners of the project, at their facilities in the industrial standard conditions. The dimensional changes of all the parts and their anisotropy are presented in this paper and discussed in relation to green density and geometry for the various materials. Particular attention is paid to the analysis of the anisotropy, not only between the compaction direction and the compaction plane but also in the compaction plane, since the latter might request a refinement of the model used for the design procedure.

2. Experimental Procedure

All the samples were produced by the industrial partners in their manufacturing facilities plants in the typical conditions of the industrial production: uniaxial double action compaction followed by sintering in continuous furnaces with temperature and atmosphere adapted to the different materials. All the parts are simple rings with different dimensions. Materials were selected to cover a broad range of shrinking/swelling behavior:

- Ferritic 430L and austenitic 316L stainless steels, representative of large shrinkage;
- Cu-Cr steel and Fe-P as representative of intermediate shrinkage;
- The prealloyed 0.85%Mo low carbon steel and the diffusion bonded Ni-Cu-Mo steel as representative of slight shrinkage;
- The Cu steel and the diffusion bonded Mo-Cu steel as representative of slight swelling.

Samples were produced with various green densities for each material.

Tables 1 and 2 summarize the materials and the specimens investigated. The Geometrical Parameter is defined as given in equation (1).

$$\text{Gometrical Parameter} = \frac{h}{\frac{(\phi_{ext}-\phi_{int})}{2}} \quad (1)$$

Where h, ϕ_{ext} and ϕ_{int} are the height, the external and the internal diameter, respectively.

Table 1. Materials, nominal chemical composition, green density and expected dimensional behavior of the specimens investigated ([a] large; [b] slight; [c] very slight)

Material code	Nominal composition (wt. %)						Green density (g/cm^3)	Volume change
	Cr	Ni	Mo	Cu	P	C		
430L	18					<0.02	6.0-6.2-6.4	Shrink[a]
316L	18	10	2			<0.02	6.4-6.6-6.8	Shrink[a]
FeCrCuC	1			1		0.8	6.0-6.2-6.4	Shrink
FeP					0.45		6.8-7.0-7.2	Shrink
FeMoC			0.85			0.2	6.7-6.9-7.1	Shrink[b]
FeNiCuMoC		4	0.5	1.5		0.55	6.7-6.9-7.1	Shrink[b]
FeCuC				1.8		0.75	6.2-6.4-6.6	Swell[b]
FeCuMoC			1.5	2		0.6	6.7-6.9-7.1	Swell[c]

Table 2. Materials, nominal dimensions and geometrical parameter of the specimens investigated

Material code	Nominal dimensions (mm)			Geometrical parameter
	φ_{int}	φ_{ext}	h	
430L	36.5	46.5	5.2 - 10.4 - 15.4	1 -2 - 3
316L	50	60	5 - 10	1 - 2
FeCrCuC	30	56	25	2
FeP	50	60	5 - 10	1 - 2
FeMoC	45	55	5 - 10 - 15	1 - 2 - 3
FeNiCuMoC	45	55	5 - 10 - 15	1 - 2 - 3
FeCuC	30	56	25	2
FeCuMoC	45	55	5 - 10 - 15	1 - 2 - 3

To evaluate the dimensional changes, part dimensions were measured both in the green and in the sintered states. Nine parts were measured for each material/density/geometry combination. Measurements were performed with DEA Global Coordinate Measuring Machine (CMM) in continuous scan mode (accuracy 3.4/120 um/s according to ISO 10360-4) [22]. Clamping

configuration in the CMM measurement area allows accessing approximately all the surfaces of the rings, as shown in Figure 1. Due to the clamps, a sector of 60° of the planar and external cylindrical surfaces were skipped during scanning, while internal cylindrical surfaces were scanned completely.

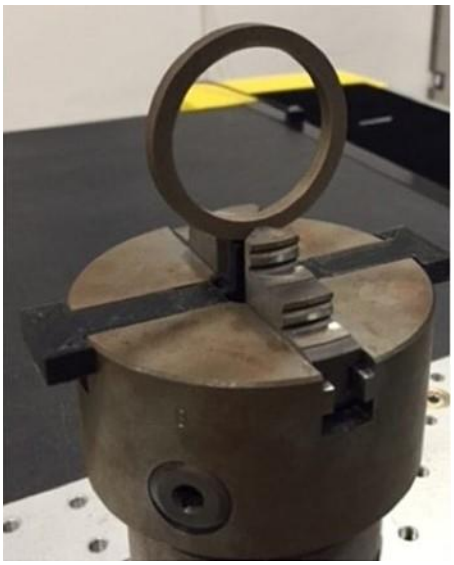

Figure 1. Example of clamping configuration

Based on previous work done by Admirabdollahian et al. [23], reference plane was set on the surface contacting the lower punch during compaction. Both internal and external circumferences were scanned at three levels at 0.25, 0.50 and 0.75 of the height, starting from upper surface. Average internal and external diameters were calculated from the reconstruction of the internal and external circumference from the data points by best fit. The dimensional changes of internal diameter ($\varepsilon_{\phi int}$), external diameter ($\varepsilon_{\phi ext}$) and height (ε_h) were calculated by equations (2), (3), (4). Also, volume change (ε_V) was calculated by equation (5), and then used to calculate equivalent isotropic dimensional change (ε_{iso}) of the samples by equation (6).

$$\varepsilon_{\phi int} = \frac{\phi_{int,s} - \phi_{int,g}}{\phi_{int,g}} \quad (2)$$

$$\varepsilon_{\phi ext} = \frac{\phi_{ext,s} - \phi_{ext,g}}{\phi_{ext,g}} \quad (3)$$

$$\varepsilon_h = \frac{h_s - h_g}{h_g} \quad (4)$$

$$\varepsilon_V = \frac{V_s - V_g}{V_g} \quad (5)$$

$$\varepsilon_{iso} = \sqrt[3]{(\varepsilon_V + 1)} - 1 \quad (6)$$

The subscripts *g* and *s* refer to green and sintered states, respectively. The volumes were calculated from internal diameter, external diameter, and height of rings with the assumption that no geometric distortion occurred during sintering.

3. Results and Discussion

3.1. Anisotropic dimensional changes

Figure 2 shows the dimensional changes of the samples as a function of green density. Data are plotted averaging the results of specimens with different geometrical parameter. In each figure, dimensional change of height, internal diameter, external diameter, and equivalent isotropic dimensional change are reported. The shrinking materials are ordered following the increase in the green density range from 430L to FeP; the two swelling materials from FeCuC to FeCuMoC.

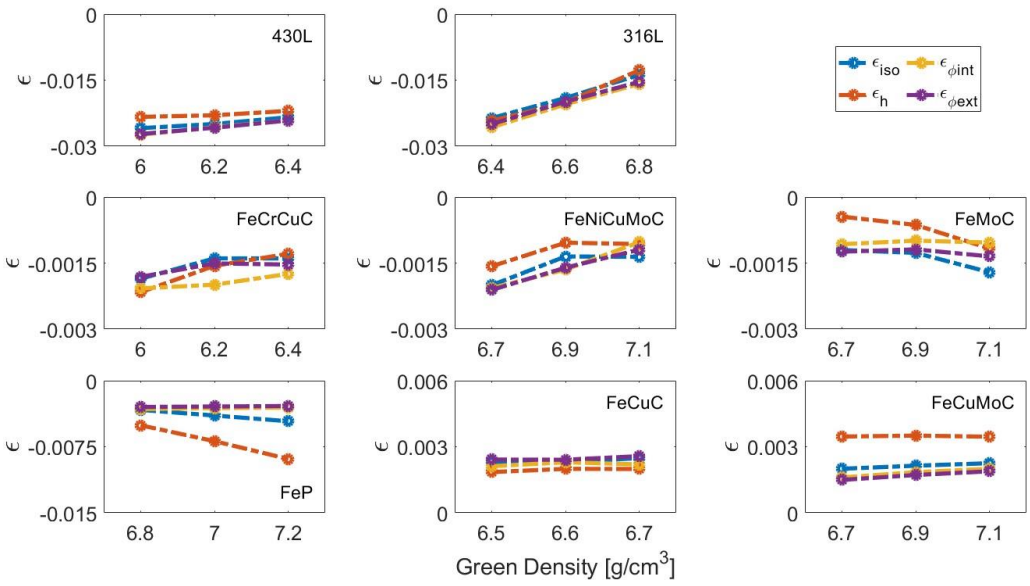

Figure 2. Dimensional changes as a function of green density (averaged on geometry)

The effect of the green density is different for the various materials. The following trends may be highlighted:

1. 430L, 316L, FeCrCuC: all dimensional changes decrease on increasing green density; height shrinkage is lower than shrinkage of diameters; the shrinkage of the two diameters is very

similar, except for FeCrCuC that displays a larger shrinkage of internal diameter than the external one.

2. FeNiCuMoC: on increasing green density isotropic and height shrinkage decrease and then slightly increase while that of diameters is almost constant; height shrinkage is smaller at low density and higher at high density than that of diameters; shrinkage of diameters is different only at the highest density.

3. FeMoC and FeP: as a general trend, shrinkage increases on increasing green density, when affected; isotropic and height shrinkage increase on increasing green density while that of diameters is almost constant; height shrinkage is slightly smaller than that of the diameters in FeMoC and the opposite in FeP; shrinkage of the diameters is very similar in FeP, while that of external diameter is larger than that of the internal one in FeMoC.

4. FeCuC: on increasing green density swelling of all dimensions and the isotropic one does not change significantly; height swells less than diameters; swelling of diameters is slightly different.

5. FeCuMoC: on increasing green density height swelling does not vary while isotropic and diameters swelling slightly increase; heights swell more than diameters; swelling of diameters is different in both the materials.

In a previous work [24] the shrinkage of iron rings was investigated. On increasing green density from 6.5 g/cm^3 up to 7.3 g/cm^3, shrinkage decreases, reaches a minimum around 6.9 g/cm^3 and increases significantly above 6.9 g/cm^3, in particular at the highest green density. This behaviour was justified considering the combined effects on dimensional change of the thermodynamic driving force of the specific surface area, that decreases on increasing green density, and of the deformation of the powder particles caused by the compaction pressure (structural and geometrical activity) that increases with green density. The former prevails at low green density, the latter at high green density and as a result shrinkage displays a minimum in correspondence of an intermediate green density. This trend may be individuated even in this work if the density ranges of the various sampling are considered. Considering the isotropic and the height shrinkage, they decrease with green density in 430L, FeCrCuC, 316L in the 6.0-6.8 g/cm^3 range; they decrease and then increase in FeNiCuMoC in the range 6.7-7.1 g/cm^3 and increase in FeP and FeMoC in the range 6.7-7.2 g/cm^3. With a good approximation it may be recognized the effect of density observed on pure iron, and the results may be still justified with the combination of the effects of

the driving force and of the deformation of the powder. The shrinkage of diameters is also coherent with the previous work, since it decreases in the low-density ranges (430L, FeCrCuC, 316L) and is almost constant in the higher density ranges (FeMoC, FeP and FeNiCuMoC).

The two swelling materials cover a broad density range, 6.5-6.7 g/cm^3 for FeCuC and 6.7-7.1 g/cm^3 for FeCuMoC. The effect of green density is rather small. It has to be taken into account that the two materials sinter in presence of a liquid phase. It is well known indeed that the increase in green density tends to enhance swelling, since the increased packing opposes a resistance to the homogeneous spreading of the liquid phase among the ferrous particles. This effect displays only in the diameters and in the isotropic swelling of the latter material, likely because green density of FeCuC parts is too low to exert a significant resistance to the spreading of the liquid phase.

In previous work [24], the effect of the geometrical parameter was less evident. On increasing the height to diameters ratio, height shrinkage decreases at the low densities and increases at the high densities, while that of diameters slightly increases. This trend cannot be observed in the present study. Figure 3 shows the dimensional changes as a function of the geometrical parameter.

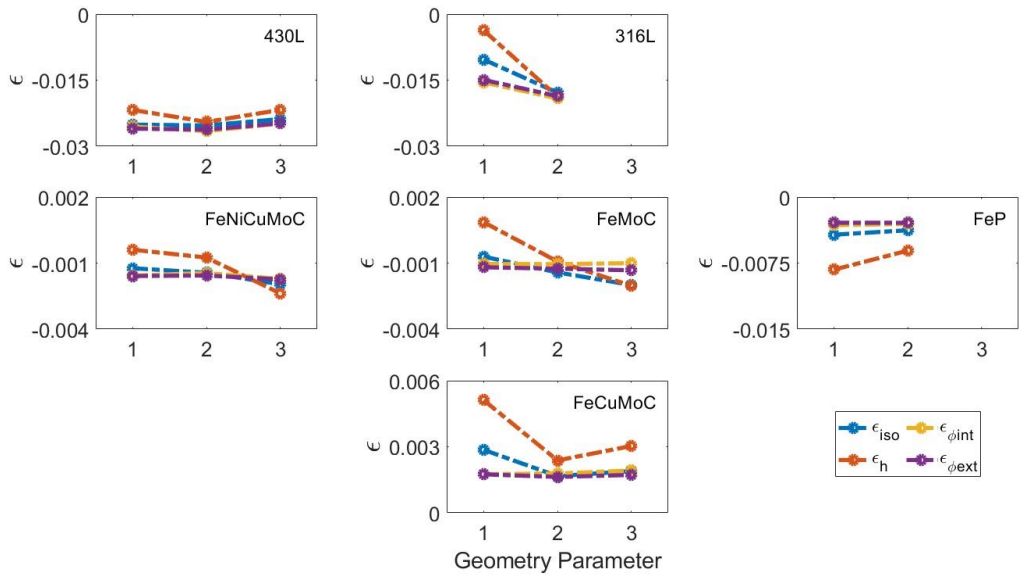

Figure 3. Dimensional changes as a function of geometrical parameter (averaged on density)

Data relevant to different densities were averaged. Among the shrinking materials, only 316L, FeMoC and FeNiCuMoC confirm the trend observed on iron, while the other two materials disagree. The only swelling material, whose data are available, shows a minimum at the intermediate geometrical parameter for height and isotropic swelling and a slightly increasing

swelling of diameters. The effect of geometry on dimensional change did not find an explanation in [24]. The trend of height may be justified considering that the compaction of the powder at the same density in a higher part requires a higher pressure [25], on the reason of frictional forces, that enhances the deformation of the powder. This effect prevails at high density, while it is overcome by that of the driving force at low density. The same phenomena should determine shrinkage of diameters, but the experimental evidence does not agree with this hypothesis neither in [24], nor in the present study. The effect of geometry on dimensional change is still subject of investigation. It is quite a complex phenomenon that depends on the compaction stresses, the compaction strategy (hold-down) and on ejection strategy, and is under investigation.

As shown in Figure 2 dimensional changes are anisotropic not only between the compaction direction (height) and the compaction plane (diameters) but also in the compaction plane since the dimensional change of the internal and external diameters are different in most cases. Figures 4 and 5 show the ratio between the dimensional change of height and the mean dimensional change of diameters ($\varepsilon_h/\varepsilon_{\phi,mean}$) and the ratio between the internal to external diameter dimensional change ($\varepsilon_{\phi int}/\varepsilon_{\phi ext}$), respectively, as a function of green density. Again, data relevant to different geometrical parameters, where available, were averaged.

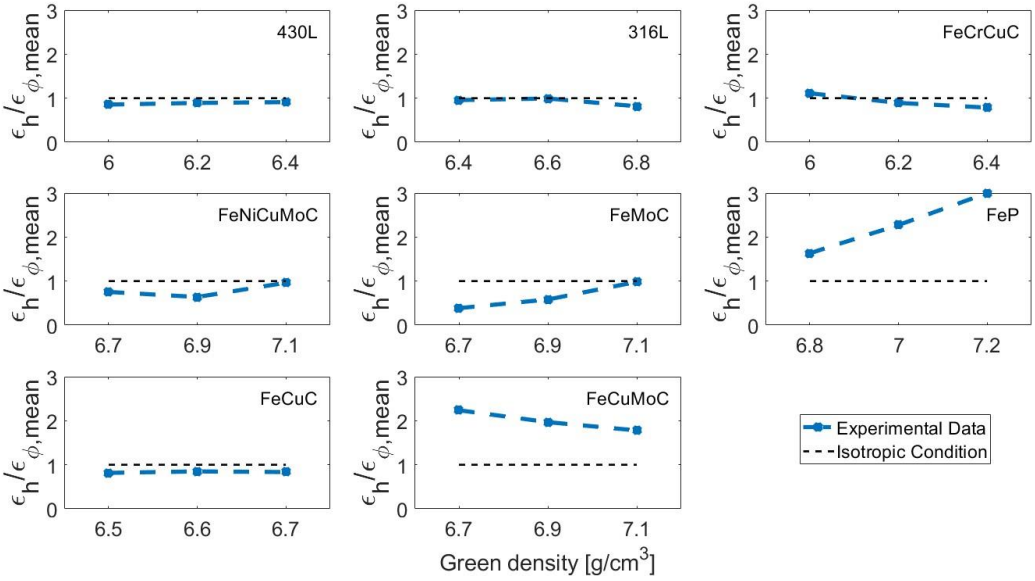

Figure 4. Ratio between the dimensional change of height and the mean dimensional change of diameters (averaged on geometrical parameter).

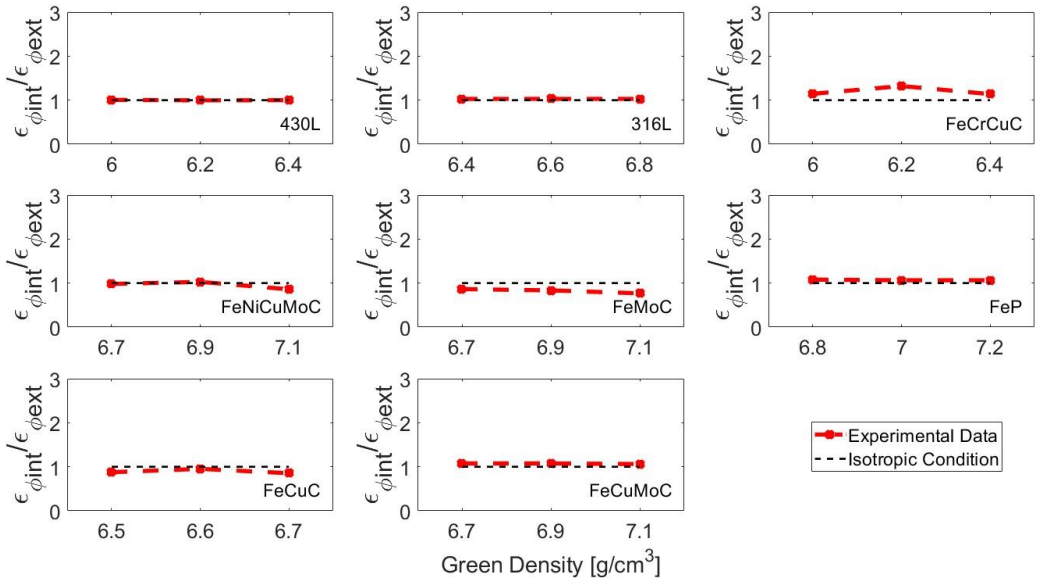

Figure 5. Ratio between the internal and external diameter dimensional change as a function of green density (averaged on geometrical parameter).

The anisotropy between the height and diameters dimensional change is very pronounced, with the exception of the two stainless steels that display the greater shrinkage among the investigated materials. This result confirms what observed in our previous studies: anisotropy of dimensional change decreases on increasing shrinkage [19]. In most of the cases dimensional change of height is smaller than that of diameters; only in FeP and FeCuMoC, height shrinks (swells, respectively) more than diameters. Green density does not have a systematic effect.

Anisotropy in the compaction plane is less pronounced. The smallest anisotropy is still observed in the two stainless steels. The effect of green density is almost negligible in the three materials that display the larger shrinkage, while in the others it is not monotonic.

Figure 6 shows the two anisotropy parameters of figures 4 and 5 as a function of the geometrical parameter, averaging the data relevant to different densities. The anisotropy does not depend on the geometry of the parts directly.

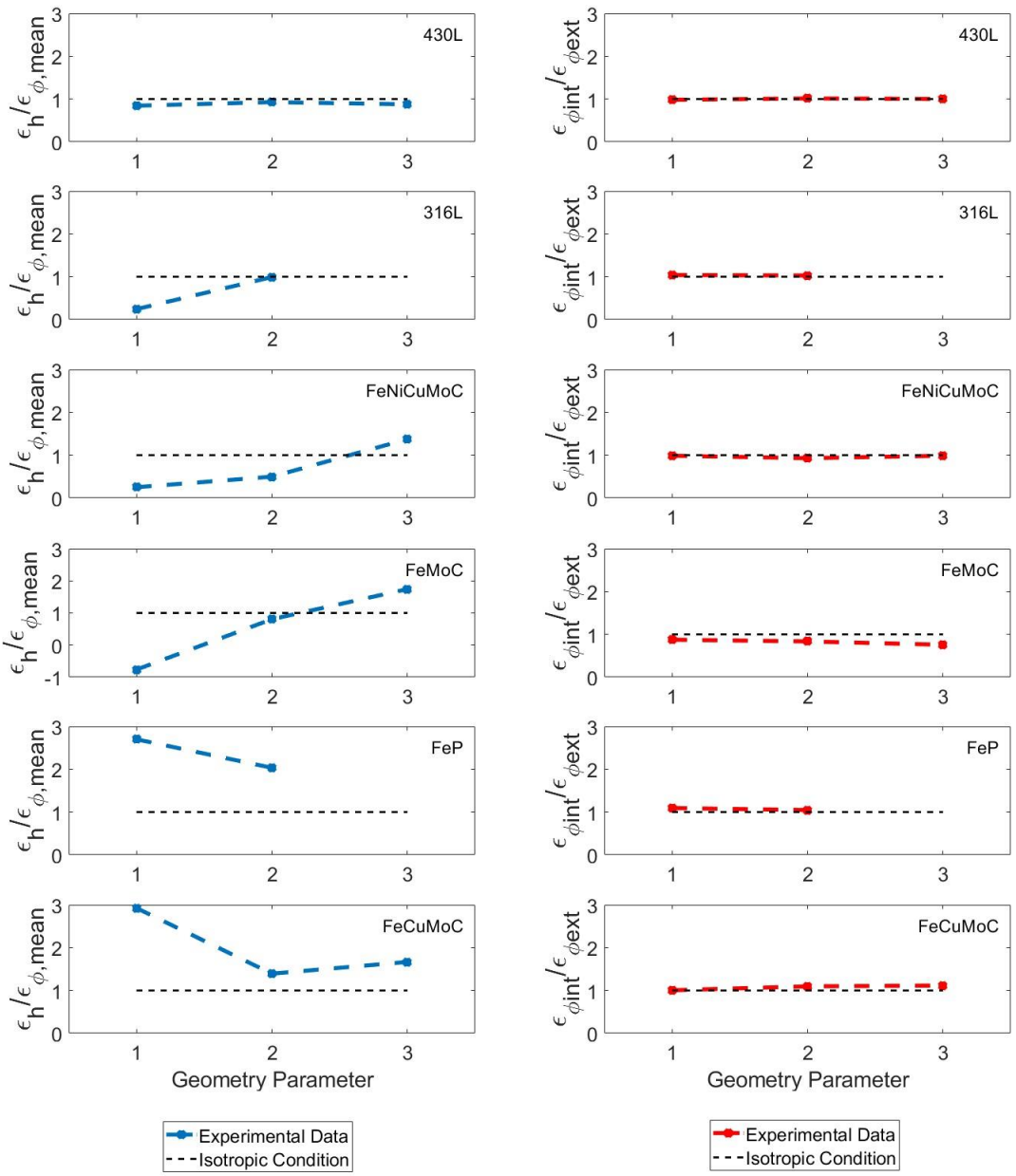

Figure 6. Ratio between the dimensional change of height and the mean dimensional change of diameters and between the internal and external diameter dimensional change as a function of the geometrical parameter (averaged on green density).

While the anisotropy between the dimensional change of height and of diameters has been subject of many investigations and different hypotheses have been proposed for its interpretation, as reported in the Introduction, the different dimensional change between the two diameters does not find references in the literature. In our previous work [24] it has been attributed to the combined

effect of the inhomogeneous distribution of the filling height in the die cavity and of green density. The distribution of height in the die cavity depends on the die filling strategy, on the powder flowability and on the part geometry. There is no clear analysis of this phenomenon yet, and studies are in progress to investigate the anisotropy in the compaction in parts produced with different process strategies and parameters.

3.2. Determination of anisotropy

Aiming at increasing the effectiveness of the production process, it is important to be able to predict the dimensional changes on sintering, to design parts properly and produce parts with high precision. First step towards a prediction model is to determine the anisotropy. In a previous work [19], the anisotropy parameter K defined by equation (7) was proposed.

$$K = \frac{\sqrt{\frac{(1+\varepsilon_{\phi ext})^2 - R^2(1+\varepsilon_{\phi int})^2}{1-R^2}} - (1+\varepsilon_{iso})}{\varepsilon_{iso}} \qquad (7)$$

where;

$$R = \frac{\phi_{int,g}}{\phi_{ext,g}} \qquad (8)$$

The design procedure proposed in [20,21] starts from the correlation between K and the isotropic dimensional change. Figure 7 shows this correlation for all the specimens of the present work, also highlighting a critical point, given that the same K value represents very different situations, both shrinking and swelling.

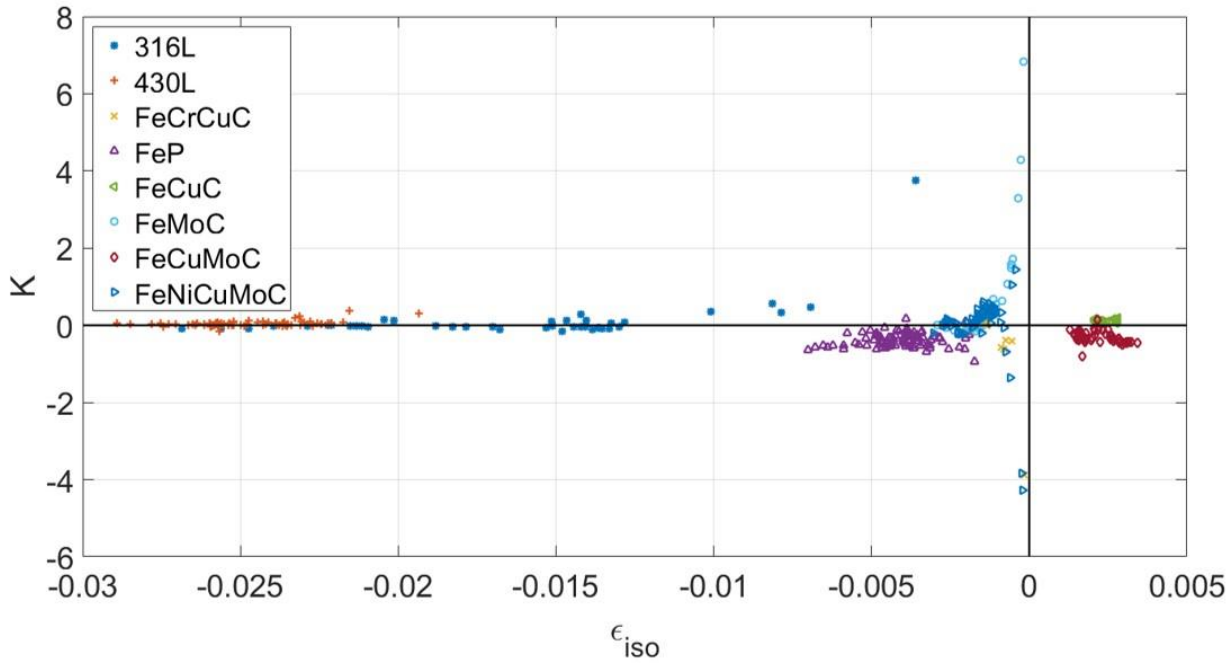

Figure 7. K vs ε_{iso}

While the anisotropy parameter has been found to be working in the previous works, current investigation highlighted some critical aspects, mainly related to the anisotropy in the compaction plane, as shown in figure 8. Here K was calculated for all the possible combinations of:

a) isotropic shrinkage, from -0.5% to -1.8%;

b) anisotropy between the height and the internal diameter shrinkage, from 0.85 to 1.15;

c) anisotropy in the compaction plane, as by different ratios between the internal and the external diameter shrinkage from 0.9 to 1.1.

The isotropic dimensional change in the compaction plane is represented by the grey curve, the isotropic shrinkage in the volume by its intersection with the X axis.

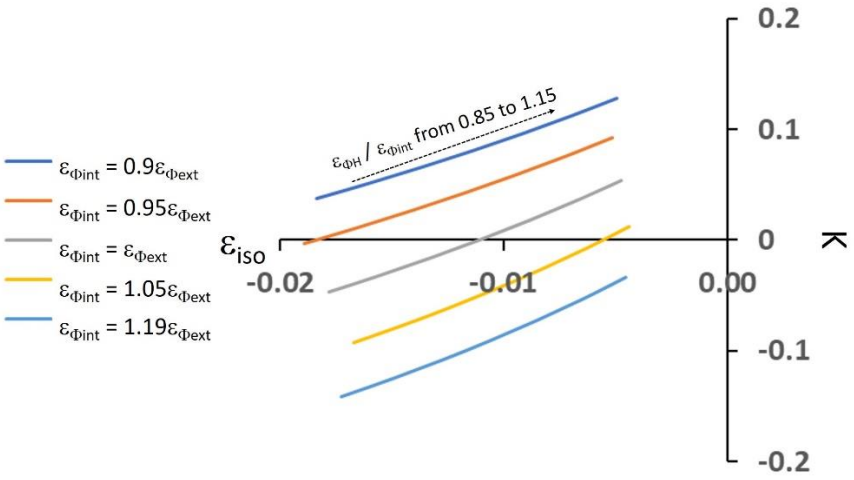

Figure 8. K as a function of the isotropic dimensional change for different ratios between dimensional changes.

Considering the condition of isotropic dimensional change in the compaction plane, K increases from negative to positive values when the height to internal diameter shrinkage increases from 0.85 up to 1.15, being equal to 0 in case of isotropic shrinkage. When the dimensional change in the compaction plane is anisotropic, the curves shift upwards and downwards, depending on whether internal diameter shrinks less or more than external diameter, respectively. Key point is that K may assume the same value for different combinations of the three-dimensional changes and may be zero even in case of anisotropic dimensional change. This confirms that K is not suitable to describe anisotropy of dimensional change when such an anisotropy displays even in the compaction plane.

The anisotropy of dimensional change in the compaction plane is very small in 430L and 316L and larger in the other materials. The external and internal dimensional changes differ by a maximum of 10%. Could such an anisotropy be neglected, the design process would result much easier. An estimation about the error introduced by neglecting the compaction plane anisotropy was made by calculating the ISO IT tolerance class corresponding to the error introduced by neglecting a difference from 2% up to 10% of the dimensional change. Figure 9 reports the ISO IT class for a nominal sintered diameter of 10mm and 50mm, its actual shrinkage ranging between 0.1% and 2% and the difference between the actual and the assumed shrinkage between 2% and 10%.

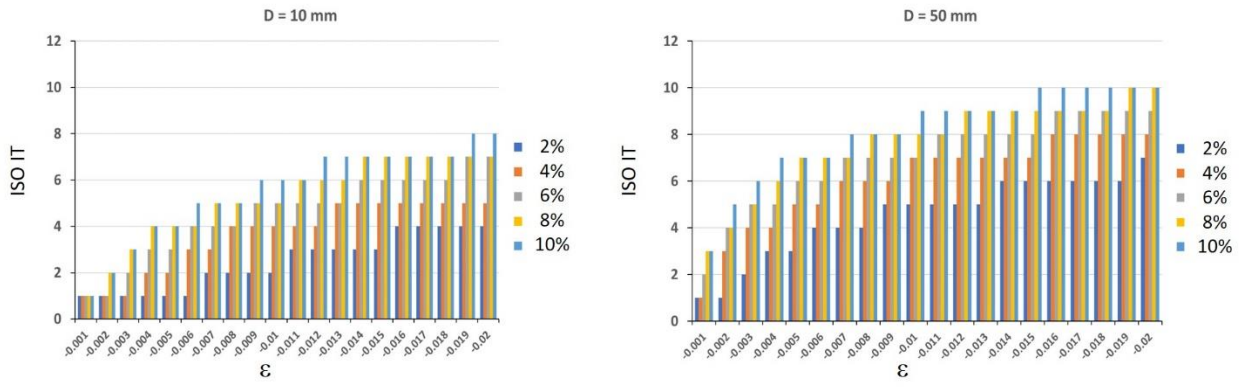

Figure 9. ISO IT tolerance class corresponding to the a 2%-10% difference of shrinkage of two nominal dimensions: 10mm and 50mm. Actual shrinkage in the abscissa.

The figure shows that the lack of precision increases on increasing the actual shrinkage, the difference between the actual and the assumed shrinkages and the nominal dimension. Considering that the typical precision of dimensions in the compaction plane of a press-and-sintered part corresponds to ISO IT6-IT7 as a result of the process capability, the figure shows that only in a very few cases the anisotropy in the compaction plane may be disregarded.

The same results were obtained considering swelling during sintering.

A new anisotropy parameter accounting for the anisotropy of dimensional change in the compaction plane is therefore necessary. The previous K anisotropy parameter was defined with reference to the distance in the cartesian plane between a point representing isotropic condition and a point representing anisotropic condition. In the cartesian plane the dimensional changes in the compaction plane were related to a parameter on the y-axis and the dimensional change in the axial direction was related to a parameter in the x-axis [19]. The new anisotropy parameter (K_{3D}) is defined with reference to the distance between the isotropy point and the anisotropy point in the 3-D space.

The distance D_{3D} between the two points is calculated by equation (9).

$$D_{3D} = |A - I| = \sqrt[2]{\left(\varepsilon_{\phi int} - \varepsilon_{iso}\right)^2 + \left(\varepsilon_{\phi ext} - \varepsilon_{iso}\right)^2 + \left(\varepsilon_h - \varepsilon_{iso}\right)^2} \qquad (9)$$

It was calculated for all the rings measured and plotted as a function of the isotropic dimensional change in Figure 10.

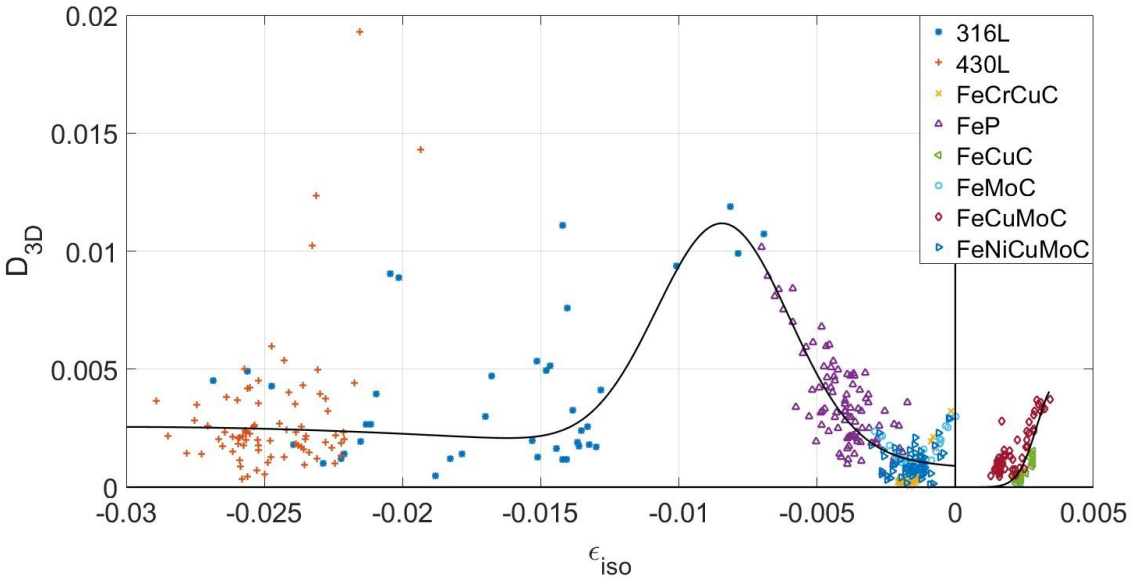

Figure 10. D_{3D} as a function of the isotropic dimensional change

The trend can be approximated by 2-term Gaussian functions, one for shrinking systems and one for swelling systems, as by equation (10).

$$D_{3D} = A_1 e^{-\left(\frac{\varepsilon_{iso}-B_1}{C_1}\right)^2} + A_2 e^{-\left(\frac{\varepsilon_{iso}-B_2}{C_2}\right)^2} \quad (10)$$

Gaussian functions are generally used for representing normal distribution, and it gives a symmetric bell curve shape when represented graphically. The parameter A is the height of the peak of the curve, the parameter B is the position of the peak, and the parameter C controls the width of the bell. The parameters are reported in Table 3.

Table 3. Fitting parameters of eq. (10)

Shrinking				Swelling	
A1	0.009712	A2	0.00255	A1	0.004364
B1	-0.008401	B2	-0.03011	B1	0.003669
C1	0.003395	C2	0.02913	C1	0.000988
Adjusted R-square		0.69		Adjusted R-square	0.4984

The quality of the fit is poor, as shown by the R-square values, due to the large scatter of the experimental data.

The three-dimensional distance was therefore referred to the isotropic dimensional change to take into account the change in volume, also obtaining a better comparison with previous K parameter. The new anisotropy parameter K_{3D} is calculated by equation (11), as the distance between the two points divided by the isotropic dimensional change

$$K_{3D} = \frac{D_{3D}}{\varepsilon_{iso}} \qquad (11)$$

and plotted in Figure 11 as a function of the isotropic dimensional change.

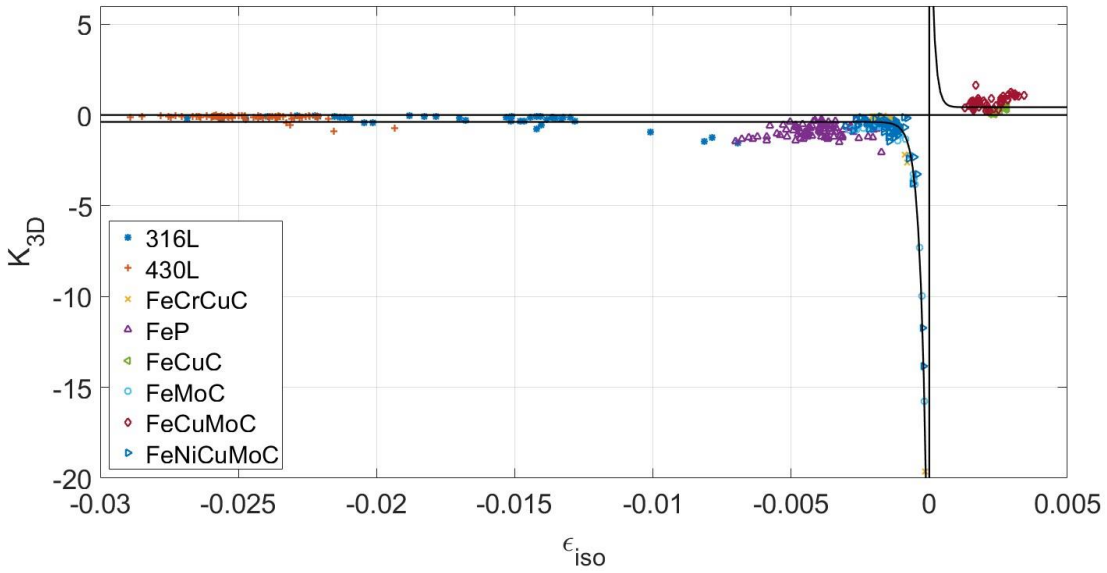

Figure 11. K_{3D}, the 3D anisotropic coefficient, as a function of the isotropic dimensional change

The trend shown in Figure 11 is similar to that shown in Figure 7, but the critical point shown in figure 7 is here solved, because there are no K values corresponding to both shrinking and swelling systems. There is a clear trend, which can be described by exponential functions, one for shrinking systems and one for swelling systems, as by equation (12).

$$K_{3D} = Ae^{B\varepsilon_{iso}} + C \qquad (12)$$

The fitting parameters are reported in Table 4, where R-square highlights the acceptable quality of the fit.

Table 4. Fitting parameters for eq. (12).

Shrinking		Swelling	
A1	-33.14	A1	15.97
B1	-4307	B1	7351
C1	-0.3819	C1	0.4283
Adjusted R-square	0.9981	Adjusted R-square	0.9849

4. Conclusions

An experimental campaign was conducted to determine anisotropic dimensional changes during sintering process. Eight different materials were considered with different green densities, and geometry parameters. Rings were cold compacted and sintered in industrial conditions. Parts were measured both in the green and in the sintered state by using a coordinate measuring machine, and dimensional changes were calculated.

The influence of green density on dimensional changes was highlighted, confirming the results obtained in previous work.

The influence of the geometrical parameter, instead, did not show clear trend, and needs for further investigation.

The anisotropy parameter K defined in previous work was calculated, but critical points were highlighted, showing the same K parameter corresponding to both shrinking and swelling systems. The result was related to the anisotropy in the compaction plane.

A new anisotropy parameter (K_{3D}) is proposed, considering the dimensional changes of internal diameter, external diameter, and height. A clear trend for K_{3D} is observed with respect to equivalent isotropic dimensional change.

Investigations to determine the relationships between dimensional changes of internal diameter, external diameter, and height are ongoing, which would lead to development of a predictive model for the anisotropic dimensional change during sintering process.

References

1. Cristofolini I, Menapace C, Cazzolli M, Rao A, Pahl W, Molinari A. The Effect of Anisotropic Dimensional Change on the Precision of Steel Parts Produced by Powder Metallurgy. J Mater Proc Techn. 2012;212(7):1513-1519.
2. Wakai F, Shinoda Y. Anisotropic sintering stress for sintering of particles arranged in orthotropic symmetry. Acta Mater. 2009;57:3955–3964.
3. Wakai F, Akatsu T. Anistropic viscosities and shrinkage rate in sintering of particles arranged in simple orthorhombic structure. Acta Mater. 2010;58:1921–1929.
4. Olevsky EA, Kushnarev B, Maximenko A, Tikare V, Braginsky M. Modelling of anisotropic sintering in crystalline ceramics, Philos Mag. 2005;85:2123–2146..
5. Torresani E, Giuntini D, Zhu C, Harrington T, Vecchio KS, Molinari A, Bordia RK, Olevsky EA. Anisotropy of Mass Transfer During Sintering of Powder Materials with Pore–Particle Structure Orientation. Metall Mater Trans A. 2019;50:1033-1049
6. Zavaliangos A, Missiaen JM, Bouvard D. Anisotropy in shrinkage during sintering. Sci Sintering. 2006;38:13–25.
7. Zavaliangos A, Bouvard D. Numerical simulation of anisotropy in sintering due to prior compaction. Int J Powder Metall. 2000;36(7):59–65.
8. Molinari A, Zago M, Amirabdollhaian S, Cristofolini I. From compaction mechanics to sintering shrinkage of rings with different H/(Dext-Dint) ratio. Adv Powder Metall Part Mater. 2018;1:81-90.
9. Zago M, Cristofolini I, Molinari A. New interpretation for the origin of the anisotropic sintering shrinkage of AISI 316L rings based on the anisotropic stress field occurred on uniaxial cold compaction Powder Metall. 2019;62(2):115-123.
10. Baselli S, Torresani E, Zago M, Amirabdollahian S, Cristofolini I, Molinari A. Sintering shrinkage of uniaxial cold compacted iron: influence of the microstructure on the anisothermal and isothermal shrinkage. Powder Metall. 2018;61(4):276-284
11. Cristofolini I, Pilla M, Larsson M, Molinari A. A Doe Analysis of Dimensional Change on Sintering of a 3% Cr-0.5% Mo-X% C Steel and Its Effect on Dimensional and Geometric Precision. Powder Metall Prog. 2012;12(3):127-143.

12. Cristofolini I, Pilla M, Rao A, Libardi S, Molinari A. Dimensional and Geometrical Precision of Powder Metallurgy Parts Sintered and Sinterhardened at High Temperature. Int. J. Precis. Eng. Manuf. 2013;14(10):1735-1742.

13. Cristofolini I, Selber F, Menapace C, Pilla M, Molinari A, Libardi S. Anisotropy of Dimensional Variation and its Effect on Precision of Sintered Parts. Proc. of Euro PM 2012 Congress & Exhibition, 2012.

14. Cristofolini I, Pilla M, Molinari A, Menapace C, Larsson M. A DOE Investigation on Anisotropic Dimensional Change on Fe-C-Cu Sintering. Int J Powder Metall. 2012;48(4):37-43.

15. Wanibe Y, Yokoyama H, Itoh, T. Expansion during Liquid Phase Sintering of Iron-Copper Compacts. Powder Metall. 1990;33(1):65-69.

16. Griffo A, Ko J, German R. Critical Assessment of Variables Affecting the Dimensional Behavior in Sintered Iron-Copper-Carbon Alloys. Adv Powder Metall Part Mater. 1994;3:221-236.

17. Raman R, Zahrah T, Weaver T, German R. Predicting Dimensional Change during Sintering of FC0208 Parts. Adv Powder Metall Part Mater. 1999;1(3):115-122.

18. Danninger H. Sintering of Mo Alloyed PM Steels Prepared from Elemental Powders. II. Mo Homogenization and Dimensional Behaviour, Powder Metall Int. 1992;24(3):163-168.

19. Cristofolini I, Corsentino N, Molinari A, Larsson M. Study of the Influence of Material and Geometry on the Anisotropy of Dimensional Change on Sintering of Powder Metallurgy Parts. Int J Prec Eng Man. 2014;15(9):1865-1873.

20. Cristofolini I, Molinari A, Zago M, Amirabdollahian S, Coube O, Dougan MJ, Larsson M, Schneider M, Valler P, Voglhuber J, Wimbert L. Design for sintering club project – dealing with the anisotropy of dimensional changes in real parts. Proceedings EUROPM2018 Congress and Exhibition, Bilbao (Spain), 14-18 October 2018, ed. EPMA, Shrewsbury (UK), CD room

21. Cristofolini I, Molinari A, Zago M, Amirabdollahian S, Coube O, Dougan MJ, Larsson M, Schneider M, Valler P, Voglhuber J, Wimbert L. Design for Powder Metallurgy: Predicting Anisotropic Dimensional Change on Sintering of Real Parts. Intl J Prec Eng Man. 2019;20(4):619-630.

22. ISO 10360-4 (2000) Geometrical Product Specifications (GPS), Acceptance and reverification tests for coordinate measuring machines (CMM), Part 4: CMMs used in scanning measuring mode.

23. Amirabdollahian S, Cristofolini I, Molinari A. Coordinate Measuring Machines (CMM) In measurements of PM parts - influence of measurement strategy and data processing. Proceedings EuroPM2018. 2018. ISBN: 978-1-899072-50-7.

24. Molinari A, Zago M, Amirabdollahian S, Larsson M, Cristofolini I. Effect of geometry and green density on the anisotropic sintering shrinkage of axisymmetric iron parts. Powder Metall. 2018;61(4):267-278.

25. Molinari A, Cristofolini I, Pederzini G, Rambelli A. A densification equation derived from the stress deformation analysis of uniaxial cold compaction of metal powder mixes. Powder Metall. 2018;61(3):210-218

Fig. 1

Click here to access/download;Colour figure (print: author charge applies);figure 1.jpg

Fig. 2

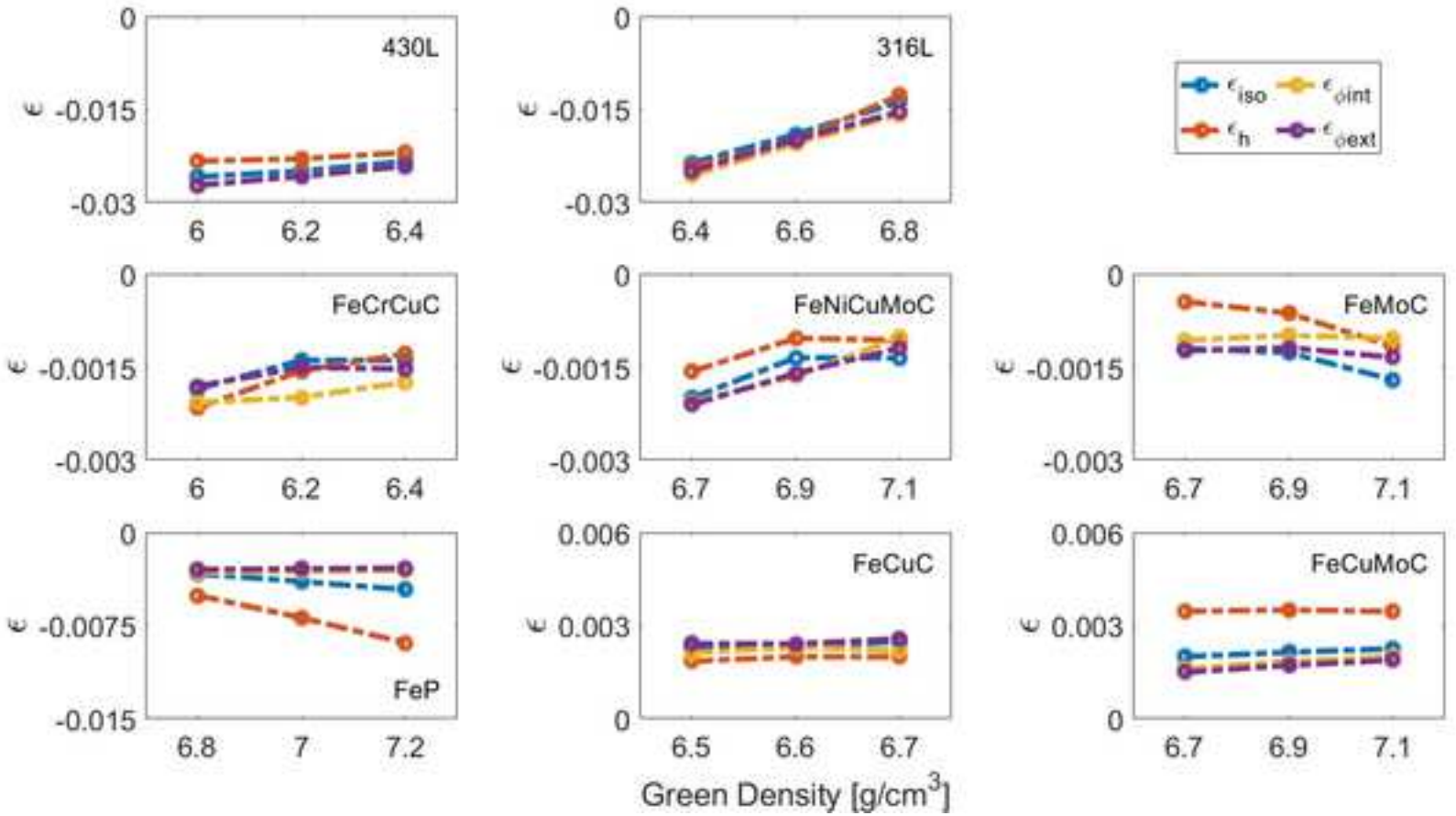

Fig. 3

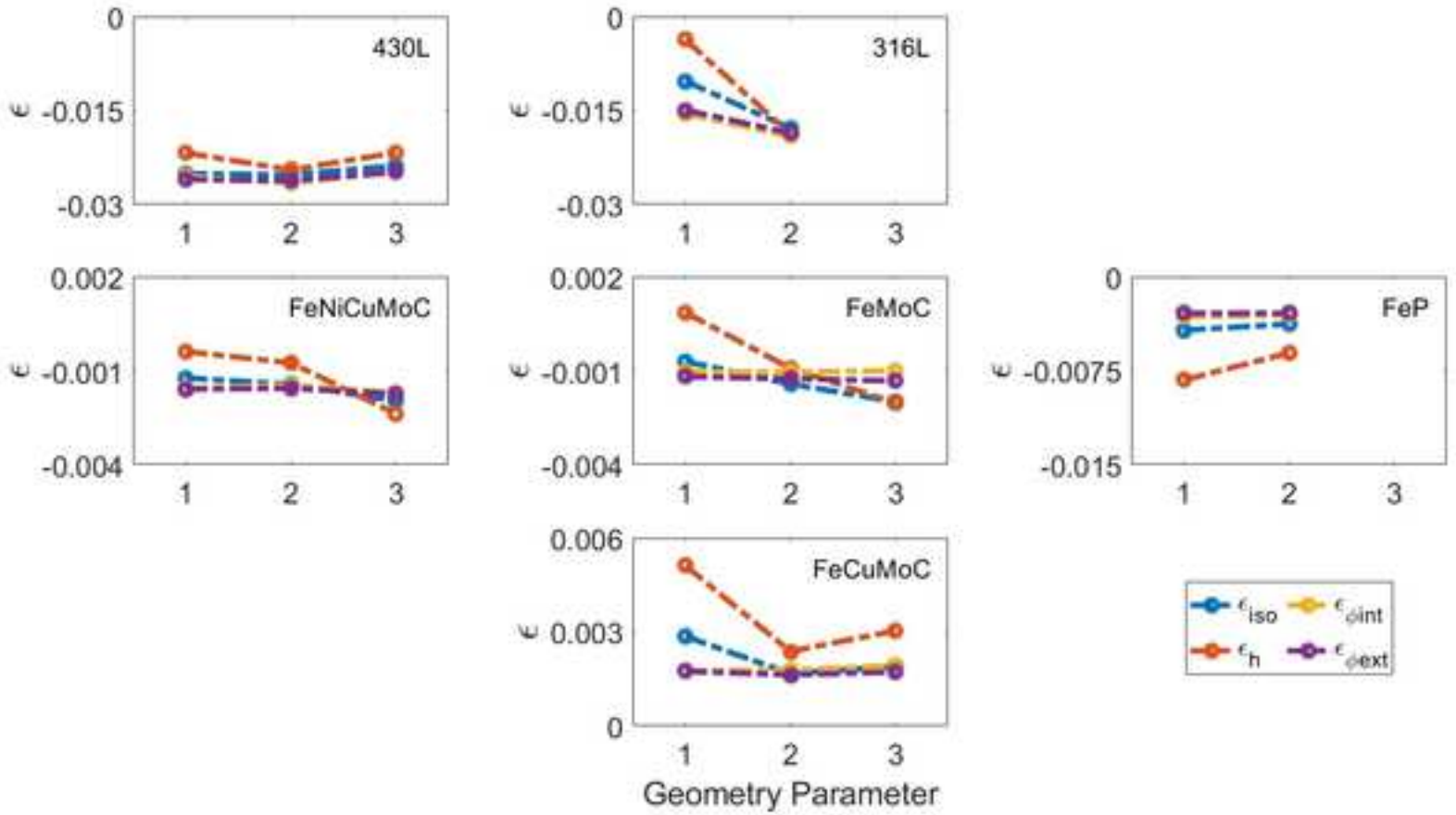

Fig. 4

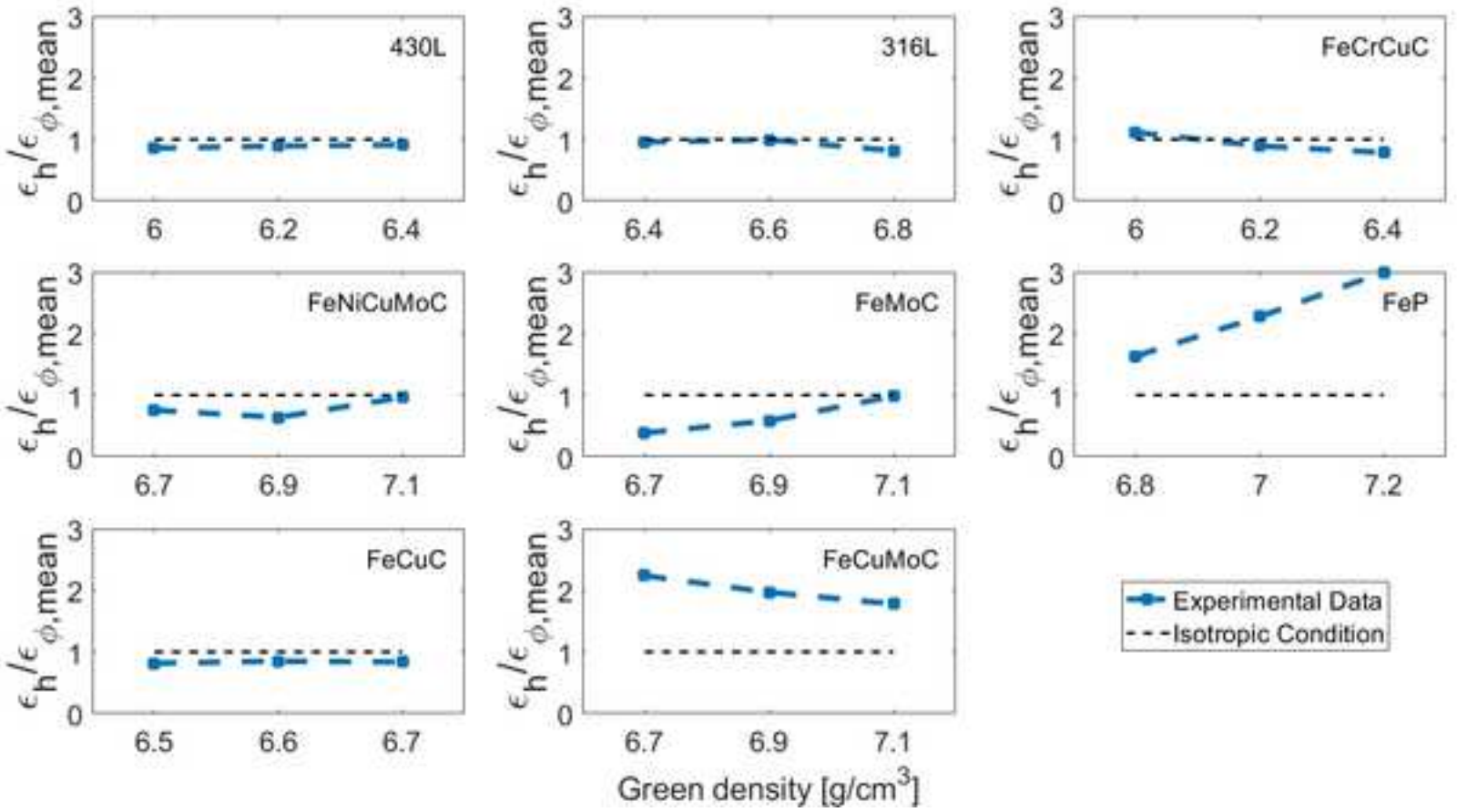

Fig. 5

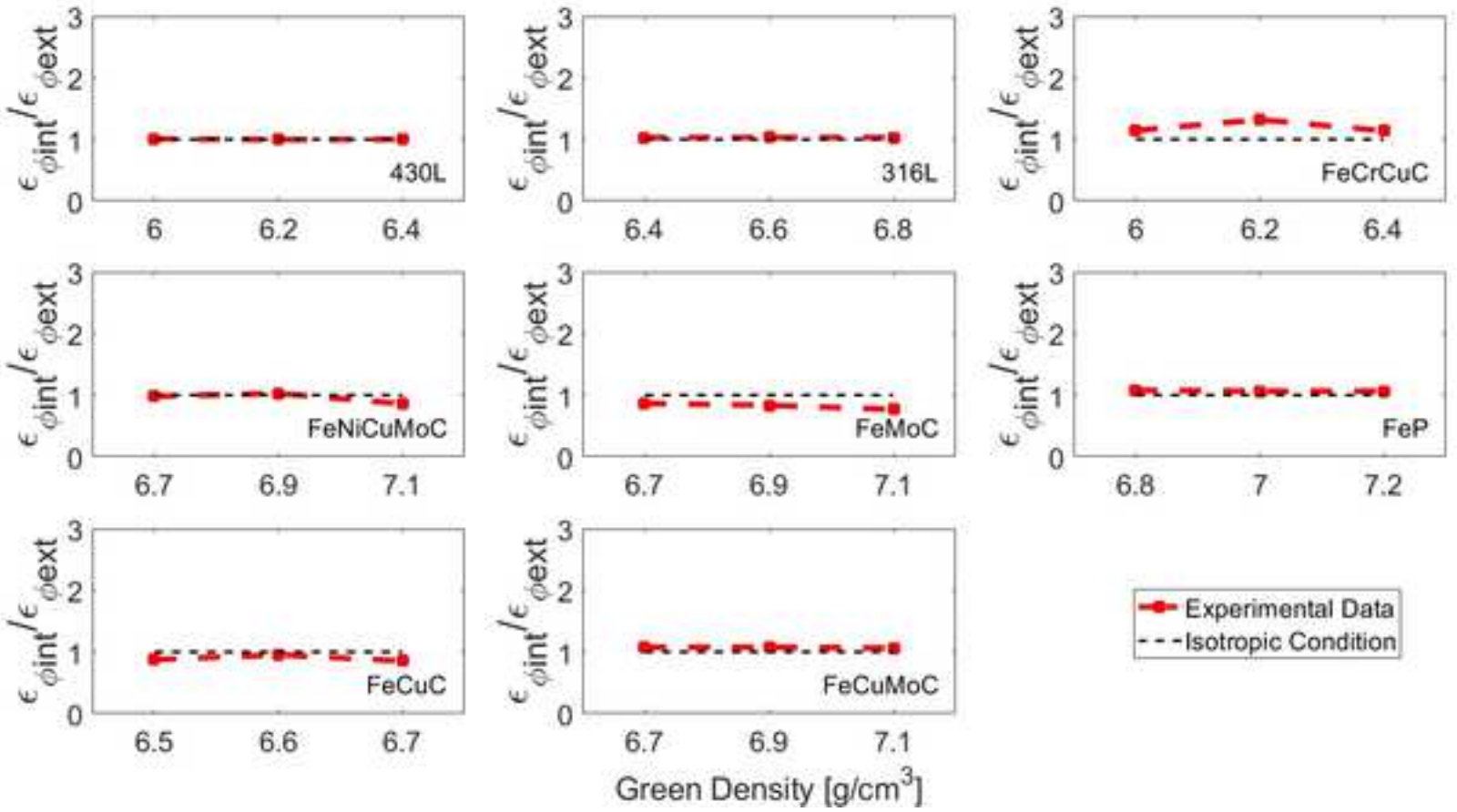

Fig.6

Click here to access/download;Colour figure (print: author charge applies);figure 6.jpg

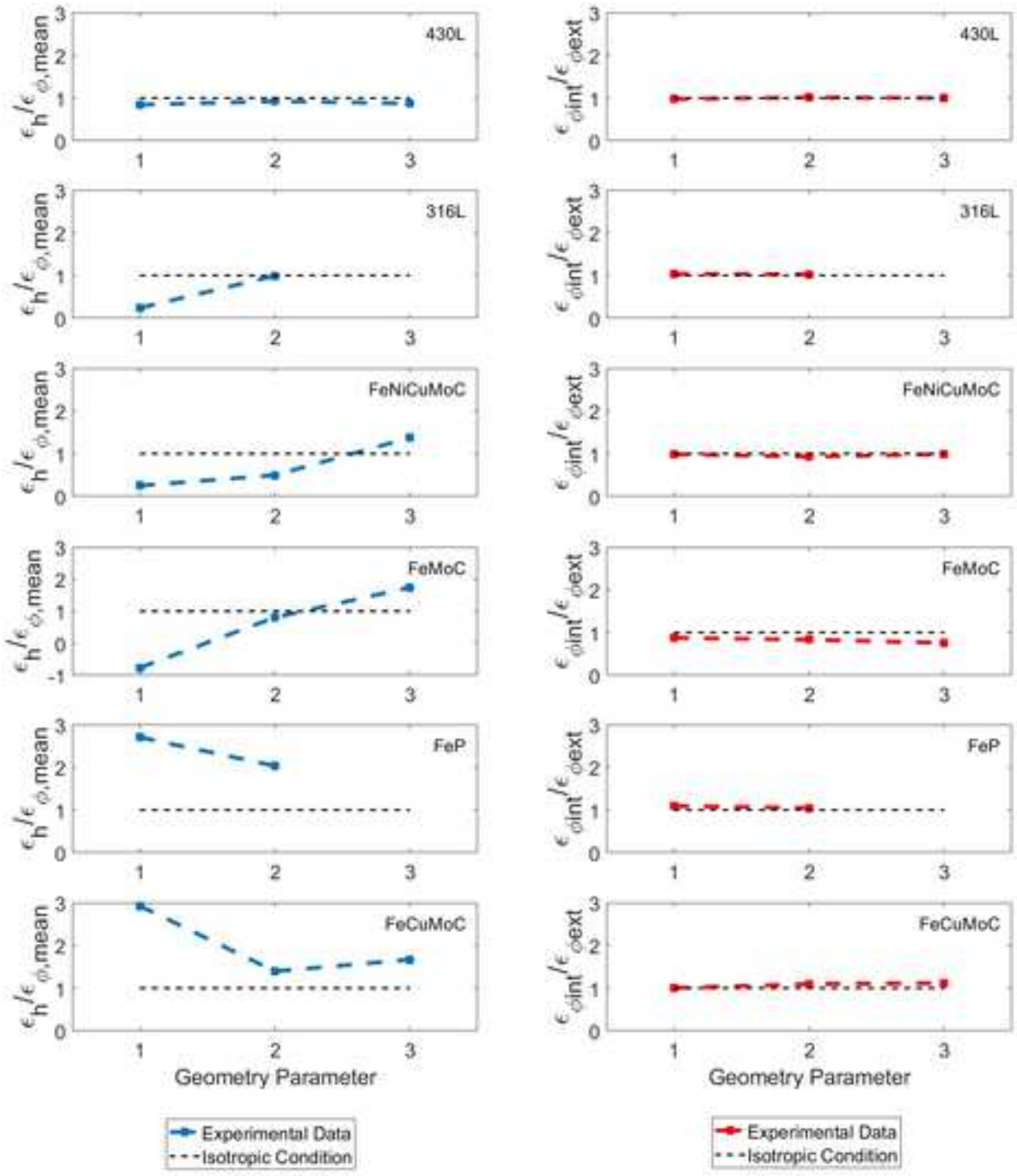

Fig. 7

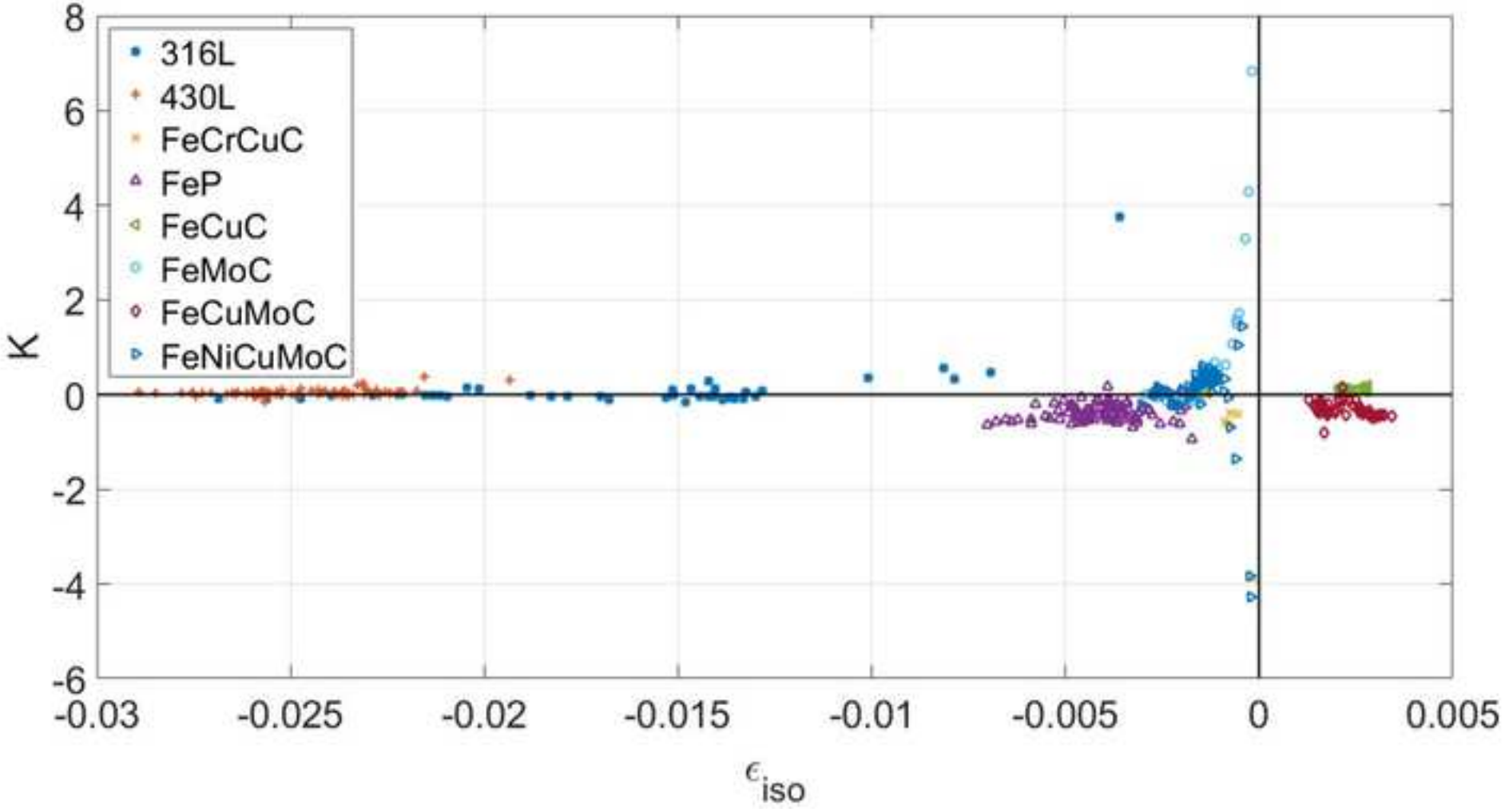

Fig. 8

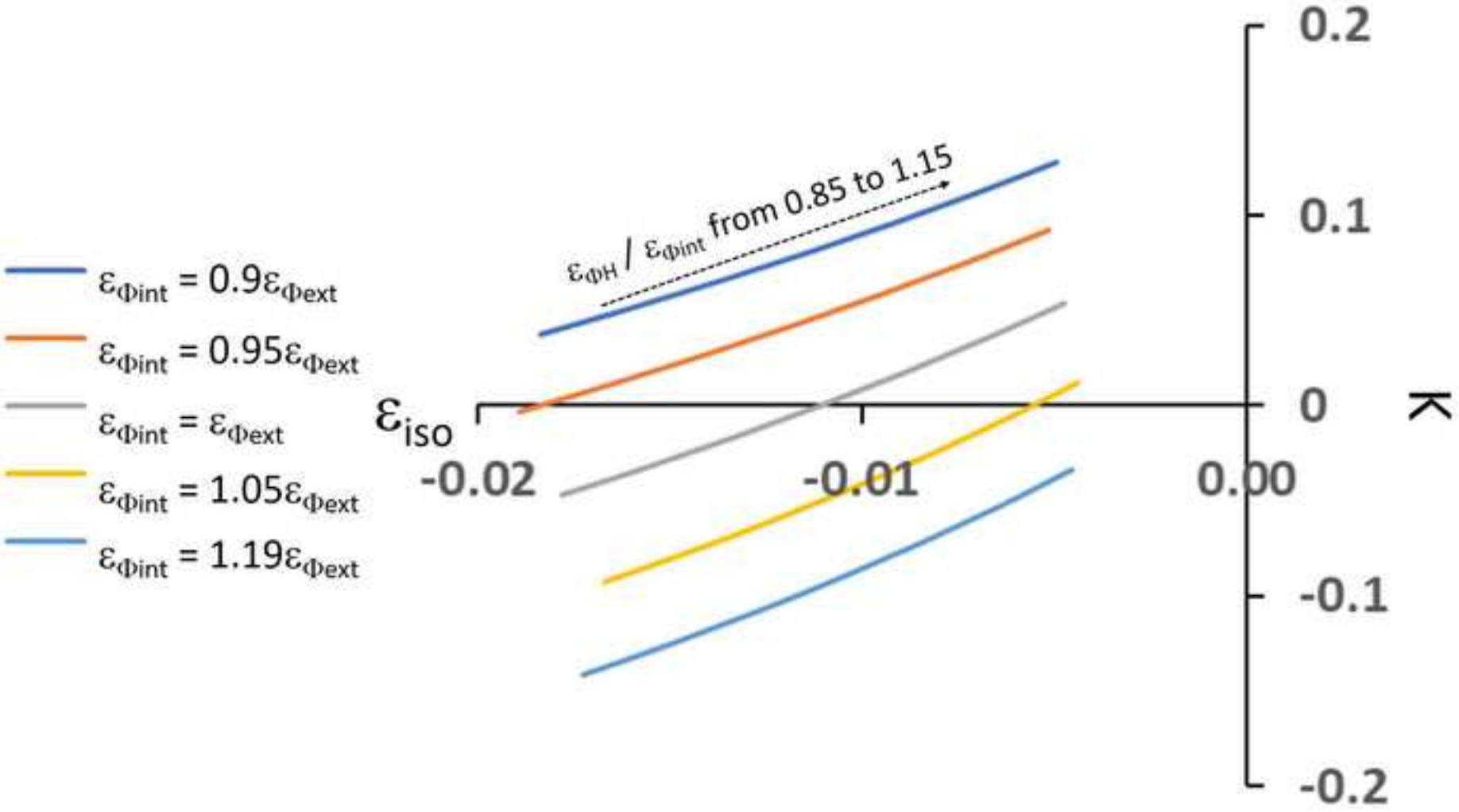

Fig. 9

Click here to access/download;Colour figure (print: author charge applies);figure 9.jpg

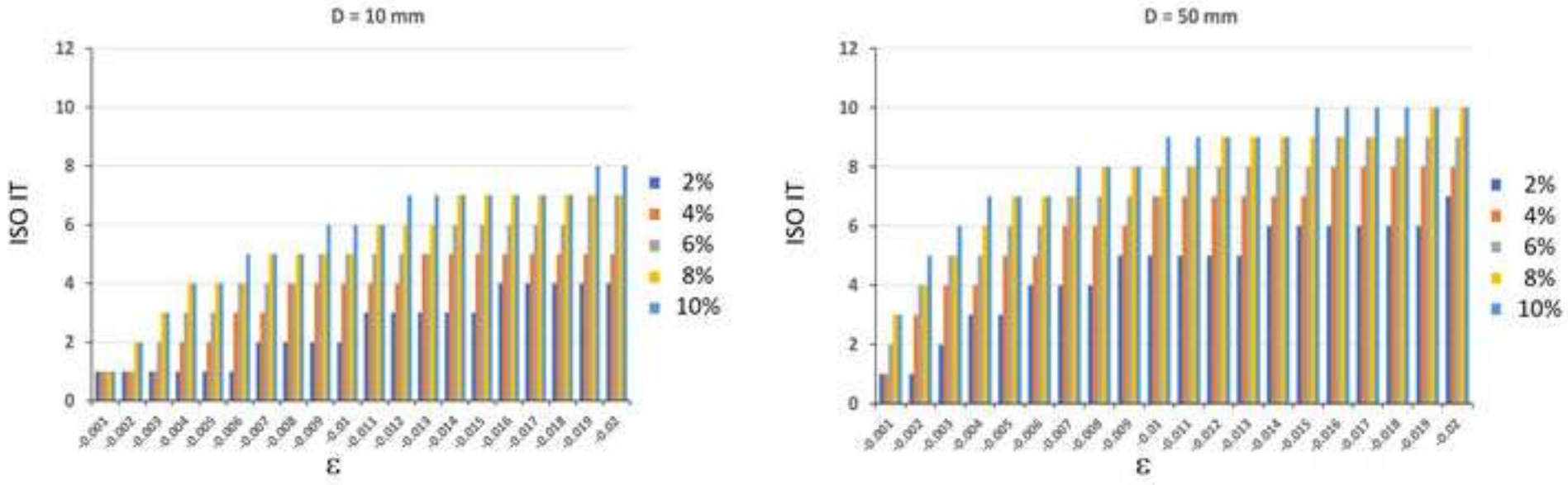

fig. 10

Click here to access/download;Colour figure (print: author charge applies);figure 10.jpg

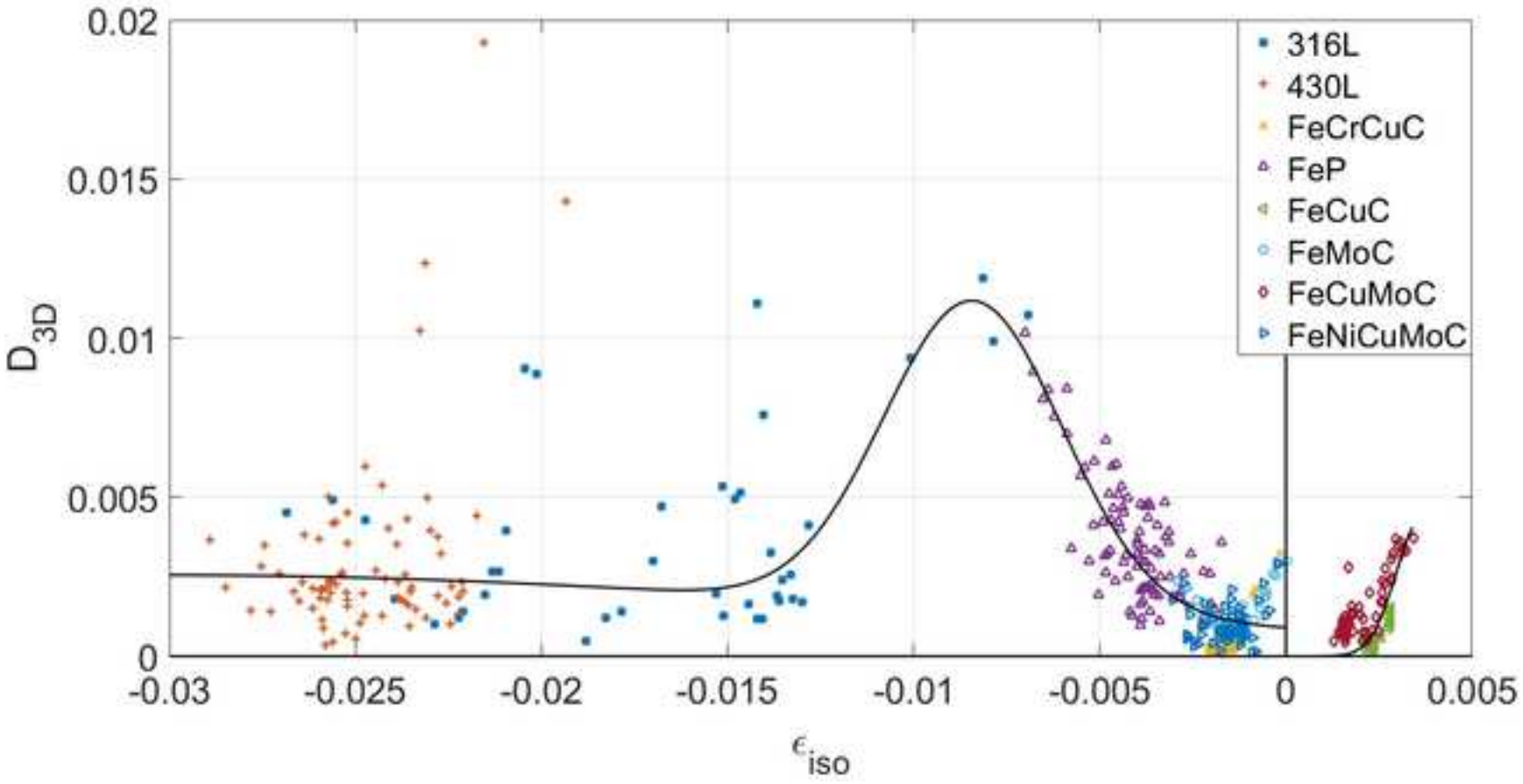

Fig. 11

Click here to access/download;Colour figure (print: author charge applies);figure 11.jpg